

Figure 1: The YSO classification scheme based on the SED shape. Our picture of the YSO formation involves the collapse of an isolated rotating dense core, forming an accreting protostellar core and a disc. The empirical evolutionary sequence goes from Class 0 to III objects. Between Class I and II an additional sub-class (Flat) has been introduced in the '90s. Class 0 YSOs are the youngest sources ($\sim 10^4$ yr), while Class III (the so-called Weak T Tauri Stars) are the oldest ones (10^7 yr). The classification of Class I, Flat, II, and III objects is based on the slope of the SED between 2 and 20μ m. Class 0 YSOs are defined as having $L_{smm}/L_{bol} > 0.5\%$, where L_{smm} is measured longward of 350μ m, and they have more than 50% of their mass in the surrounding envelope. Credits: Lada 1987; André et al. 1993; O'Connell 2005.

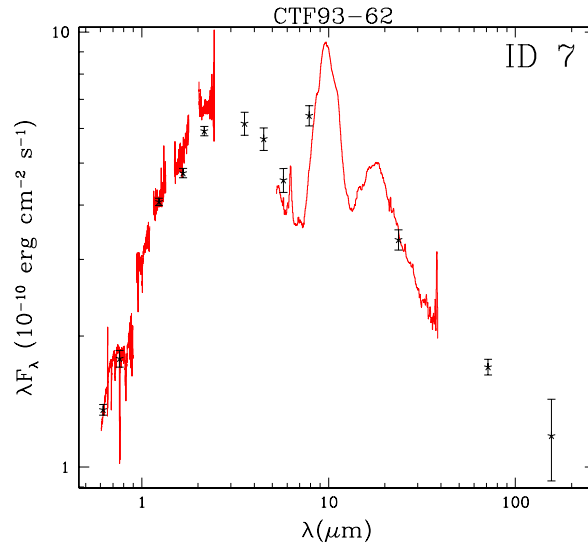


Figure 2: Example of our YSO SEDs ([CTF93]-62 in L 1641 molecular cloud), built using data photometry (in black), optical and infrared spectroscopy (in red). Credits: Caratti o Garatti et al. 2011b.

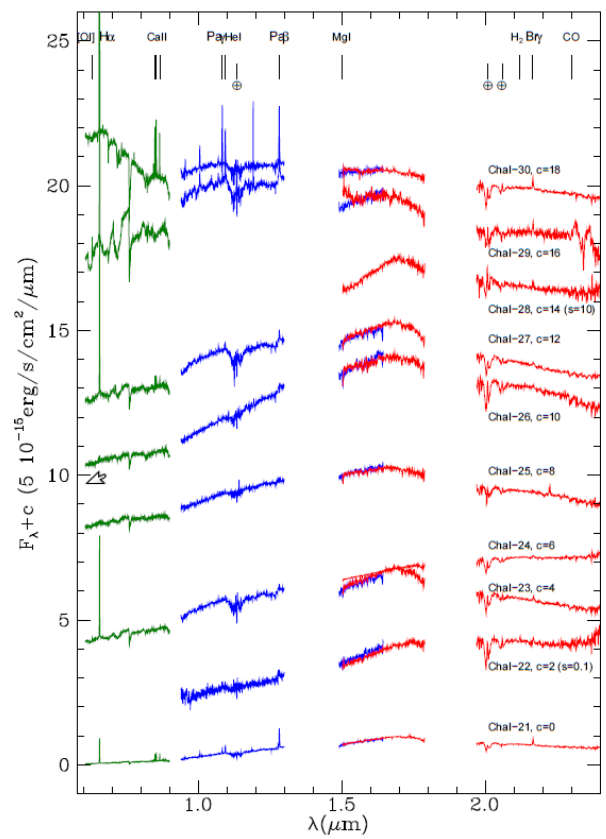
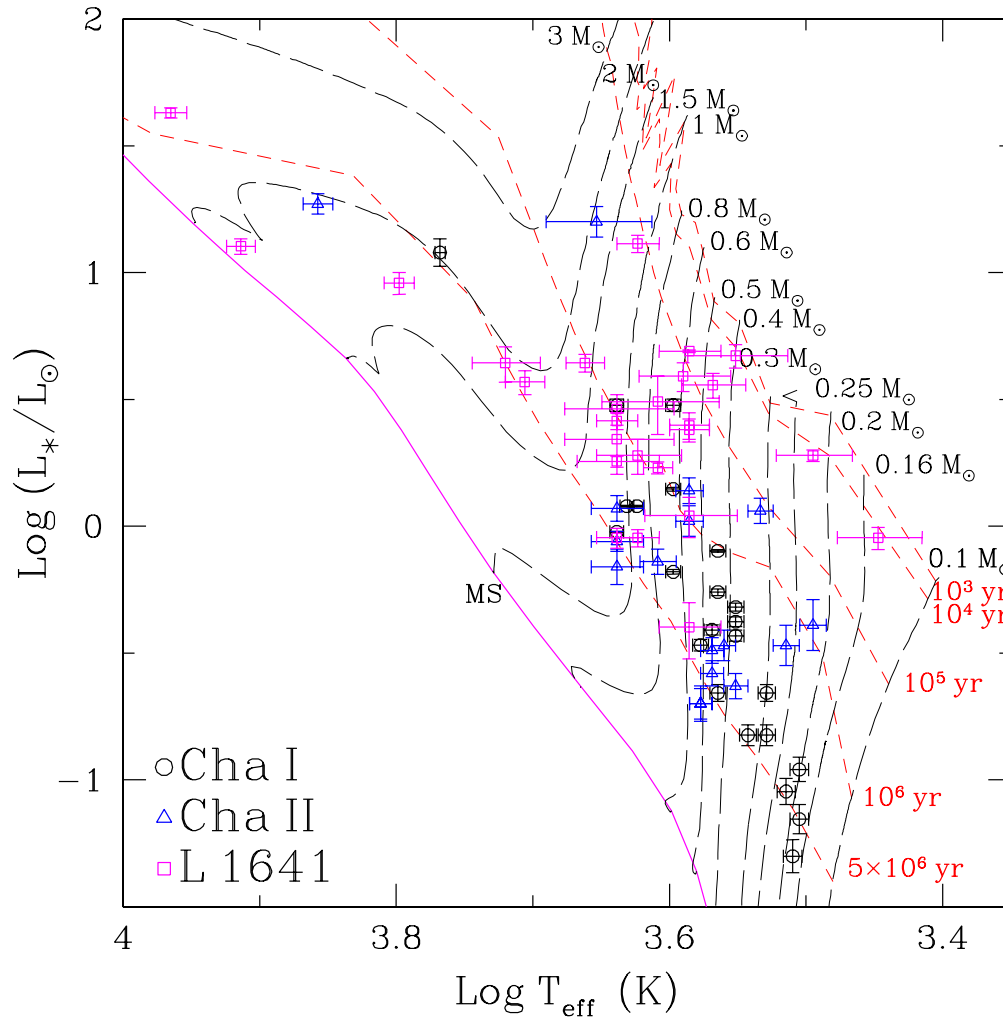


Figure 3: Examples of our optical near-infrared spectra (in Cha molecular clouds), constructed using ESO EFOSC2 (green) and SofI spectroscopy (in blue and red). The position of the main

emission lines present in the covered spectral range is indicated. *Credits: Antonucci et al. 2011.*



*Figure 4: Herzprung Russell (HR) diagram for the Cha I, II and L 1641 samples. The evolutionary models of Siess et al. 2000 are shown with isochrones at 10^4 , 10^5 , 10^6 , and 5×10^6 yr (red dashed lines), and mass tracks from 0.1 to $3 M_\odot$ (black dashed lines). *Credits: Caratti o Garatti et al. 2011b.**

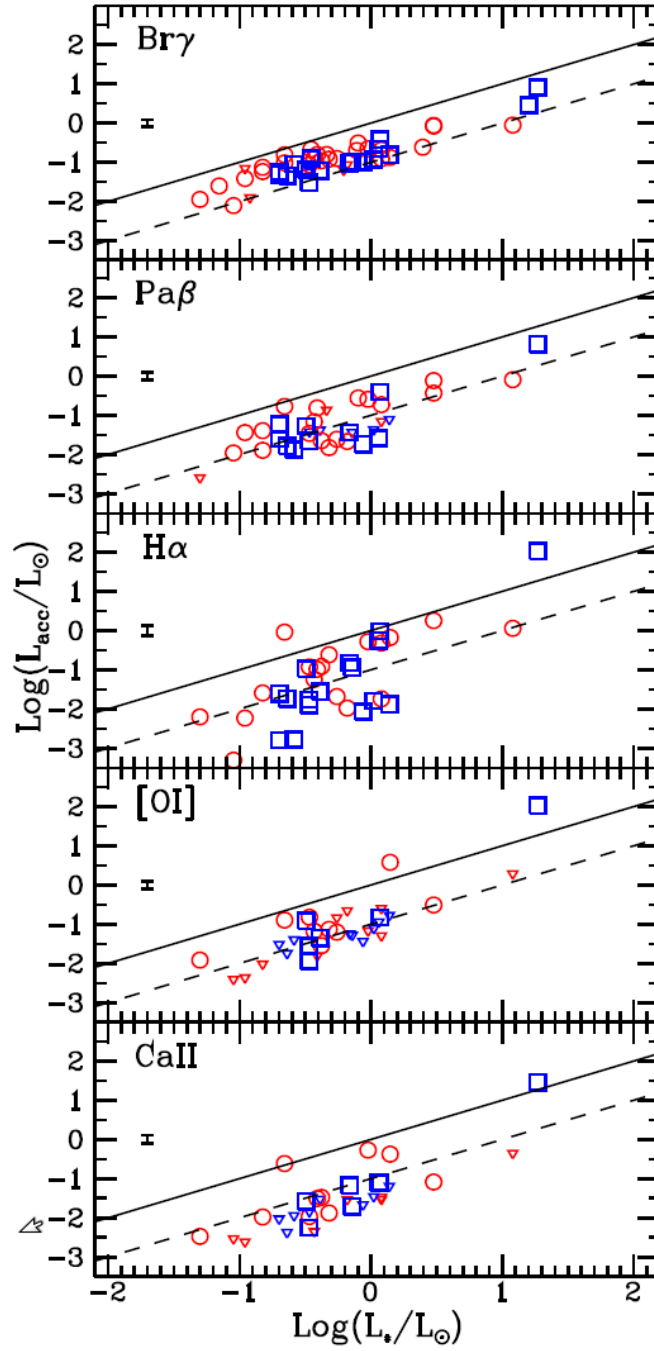


Figure 5: L_{acc} values for the different accretion tracers considered in our analysis of Cha clouds plotted as a function of L_* : from top to bottom $Br\gamma$, $Pa\beta$, $H\alpha$, $[O I]$ at 6300, $Ca II$ at 8542. Red circles and blue squares refer to detections of Cha I and Cha II objects, respectively. Upper limits are indicated by downward triangles. The solid and dashed lines show the locus where $L_{acc}=L_*$ and $L_{acc}=0.1L_*$, respectively. Credits: Antoniucci et al. 2011.

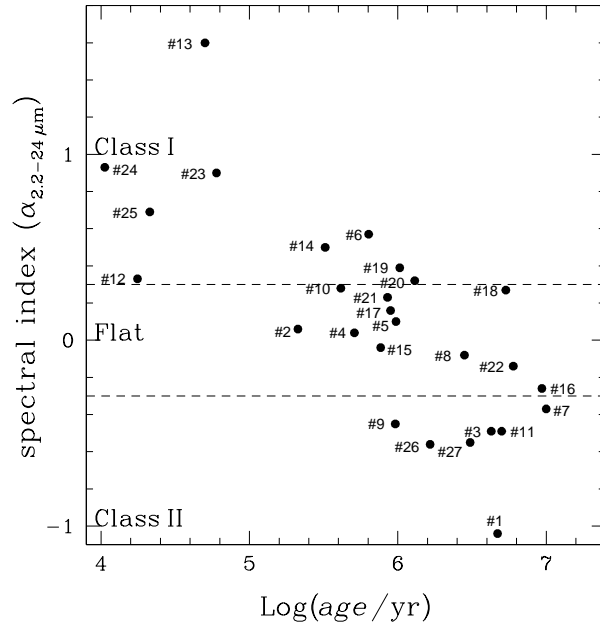


Figure 5: Spectral index (α) versus age of the YSO sample in L 1641 molecular cloud. The two dashed lines delineate the Class I-Flat ($\alpha = 0.3$) and Flat-Class II ($\alpha = -0.3$) boundaries. The plot shows that the standard SED classification (computed between 2.2 and 24 μm) does not properly reflect YSO age, i. e. that the SED slope might not be a good indicator of the stellar age. Indeed, geometrical effects may play a role in modeling the YSO SED (see e. g., Whitney et al. 2003; Robitaille et al. 2007), altering the slope and generating misclassifications. **Credits: Caratti o Garatti et al. 2011b.**

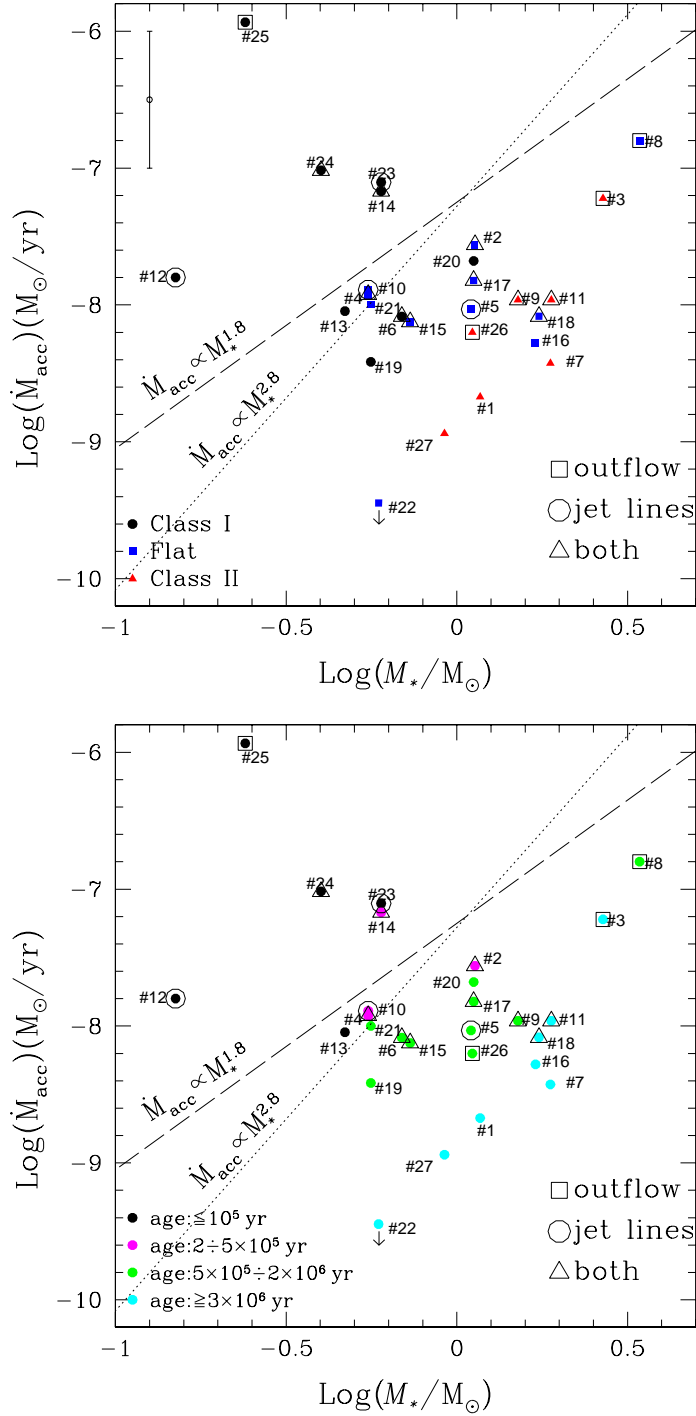


Figure 7: Upper panel: Mass accretion rate versus stellar mass for the L 1641 sample. The different symbols indicate the class of the objects: Class I, Flat, or Class II (dots, squares, and triangles, respectively), and the object IDs are also reported. The presence of jets/outflows in the images, lines tracing jets in the spectra, or both is indicated by open squares, circles, or triangles, respectively. The dashed line shows the $M_{\text{acc}} \propto M_*^{1.8}$ relationship obtained by Natta et al. 2006 for the Ophiucus sample, whereas the dotted line displays the $M_{\text{acc}} \propto M_*^{2.8}$ relationship obtained by Fang et al. 2010 for the L 1634 and the L 1641 samples. There is a marginal trend between the mass accretion rate

evolution and the YSO class.

Bottom panel: Same as top panel, with colours indicating the different age of the objects, ranging from $\leq 10^5$ to 10^7 yrs. There is a marginal trend between the mass accretion rate evolution and the YSO class. Here, there is a more clear correlation between the mass accretion evolution and the age of the YSOs. The YSO classification scheme does not properly represent the evolutionary stages of the YSOs. **Credits: Caratti o Garatti et al. 2011b.**

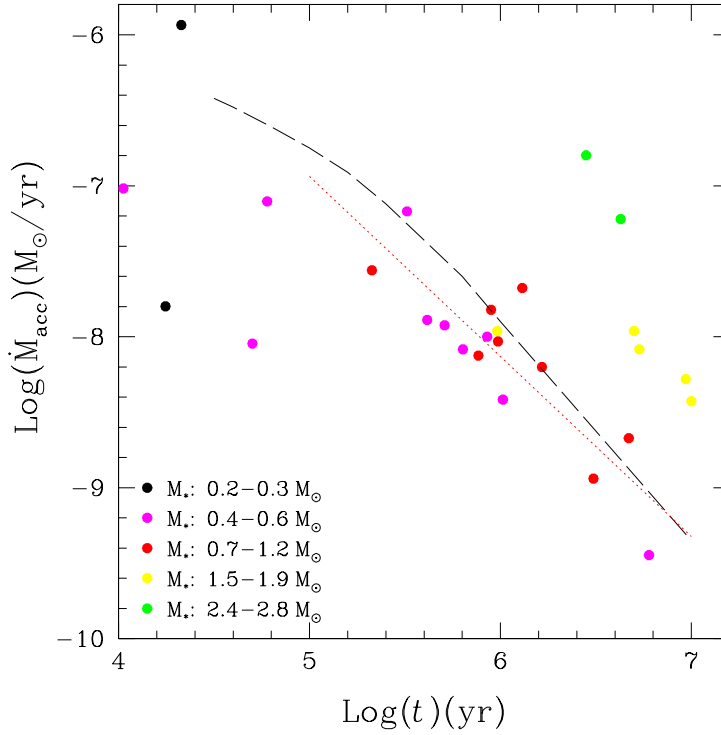


Figure 8: Mass accretion rate as a function of stellar age for the observed sample in L 1641 (Caratti o Garatti et al. in prep.). The various colours indicate the different mass ranges of the objects. The dashed line displays one of the viscous models of Hartmann et al. 1998, for a $M_* = 0.5 M_{\odot}$, an initial disc mass $\dot{M}_d = 0.1 M_{\odot}$, viscosity parameter $\alpha = 10^{-2}$, and viscosity exponent $\gamma = 1$, i. e. $\eta = 1.5$ in the $\dot{M}_{\text{acc}} \propto t^{-\eta}$ relationship. The red dotted line shows the best linear fit for data points with $0.4 \leq M_* \leq 1.2 M_{\odot}$ and $t > 10^5$ yr, i. e. during a temporal range where the viscous processes likely control the mass accretion rate. Our best fit gives $\dot{M}_{\text{acc}} \propto t^{-1.2}$. **Credits: Caratti o Garatti et al. 2011b.**

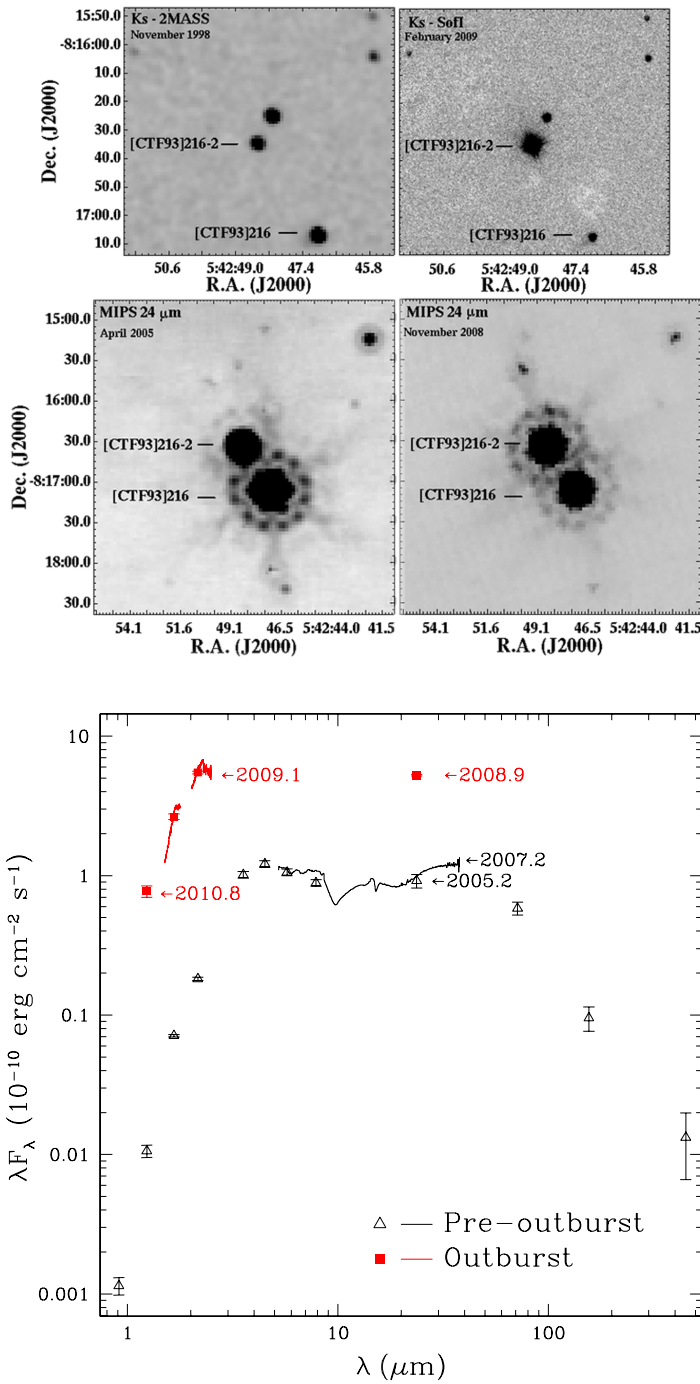


Figure 9: Upper panel: K_s (top panels) and MIPS-24 μ m (bottom panels) images of [CTF93]216-2 (the discovered outbursting YSO) and its surroundings before (left) and after (right) the outburst. The position of the YSO [CTF93]216 (its possible companion) is also indicated. Bottom panel: Spectral energy distribution of [CTF93]216-2. Pre-outburst data: black triangles (photometry), and black line (Spitzer-IRS mid-IR spectrum). Outburst data: red squares (photometry), and red line (SoFI NIR spectrum). Credits: Caratti o Garatti et al. 2011a.